

Liquid Crystal Polymer (LCP), an Attractive Substrate for Retinal Implant

Joonsoo Jeong^{1,2}, Seung Woo Lee³, Kyou Sik Min^{1,2},
Soowon Shin^{1,2}, Sang Beom Jun⁴ and Sung June Kim^{1,2,*}

¹Department of Electrical Engineering and Computer Science, Seoul National University,
1 Gwanak-ro, Gwanak-gu, Seoul 151-742, Korea

²Inter-University Semiconductor Research Center, Seoul National University,
1 Gwanak-ro, Gwanak-gu, Seoul 151-742, Korea

³Department of Neurosurgery, Massachusetts General Hospital,
Harvard Medical School, Boston, MA 02114, U.S.A.

⁴Department of Electronics Engineering, Ewha Womans University,
52 Ewhayodae-gil, Seodaemun-gu, Seoul 120-750, Korea

(Received December 9, 2011; accepted February 16, 2012)

Key words: liquid crystal polymer, retinal implant, conformable structure, planar coil, retinal prosthesis, monolithic encapsulation, soak test

Recently, there has been growing interest in liquid crystal polymer (LCP) as a new biomaterial for next-generation implantable neural prosthetic devices. LCP has a very low moisture absorption rate compared with other polymers such as polyimide or polyethylene-C, providing a superior long-term reliability in the human body. In addition, LCP film is compatible with semiconductor processes, and layer-to-layer lamination is possible simply by fusion bonding of multiple LCP sheets with heat and pressure without the use of adhesives. A monolithic system can be implemented by using LCP as the substrate of electrodes and printed circuit boards as well as packaging material. Therefore, the LCP-based system can achieve a much higher long-term reliability, while maintaining the merits of conventional polymer-based systems such as thinness, flexibility, and simple fabrication procedure. In the present study, we have shown the feasibility of LCP as a substrate and packaging material for a novel monolithic retinal prosthetic device. The patterns of printed circuits and a planar coil were formed on LCP films by thin-film processes, and eye-surface-conformable structure was achieved that enables the attachment of the whole retinal implant on the eyeball. It has been verified that the spherical deformation process did not adversely affect the electrical characteristics or the performance of the printed circuits and the planar coil. The long-

*Corresponding author: kimsj@snu.ac.kr

term reliability of LCP-encapsulation was evaluated by an *in vitro* accelerated soak test, and possible failure mechanisms were investigated. The LCP-encapsulation could provide reliable electrical insulation for ~400 days in 75°C phosphate-buffered solution (PBS).

1. Introduction

The retinal prosthesis is an implantable electronic device for restoring visual function for those suffering from partial or total blindness due to retinal degeneration such as retinitis pigmentosa (RP) or age-related macular degeneration (AMD). A number of research groups have been dedicated to developing implantable retinal prosthetic devices for efficient and safe retinal stimulation.⁽¹⁻⁸⁾ Some of them have reached the level of clinical trials, where the patients with retinal prostheses could perceive phosphenes that correspond to the location and strength of the electrical stimulation.^(9,10)

The retinal prosthetic systems to date are mostly based on the previous technologies of metal hermetic packages, silicone rubber coatings, and additional transmission wire coils, which have been used for other neural prosthetic devices such as cochlear implants or deep brain stimulation systems. The next-generation retinal prostheses are expected to be smaller, thinner, simpler to fabricate, and more reliable for stable and efficient chronic operation. For implantable biomedical devices, in general, the slim size and flexibility are undoubtedly beneficial. In particular, a small size of the implanted device is critical for the retinal implant compared with other neural prosthetic systems, since the electrode array, the packaged circuitries, and coils are desired to be fixed on the surface of the eyeball. The anatomically available space around the eye is very limited and the risk of infection and device failure is high as a result of the continuous movement of the eyeball. A conformable structure that fits the implantation environment is also highly required.

Titanium and ceramic have been most commonly used for the packaging materials of the implantable systems to protect the stimulator circuitries from moisture and salts inside the body. However, they are relatively bulky and incompatible with semiconductor processes. They also have several limitations, for example, the production cost is high owing to the need for manual work, and the feedthrough technologies are required, limiting the number of channels, which are crucial for high-density neural stimulation.

Because of these disadvantages, polymer-based neural prosthetic devices have been actively explored to replace the metal and ceramic packages of mostly polyimide and parylene-C.^(4,11-13) Whereas the packages and the microelectrode arrays based on polymer materials are thin, flexible, and compatible with microfabrication processes, the reliability of long-term implantation remains questionable owing to their high moisture absorption rate and the insufficient interlayer adhesion strength resulting in degradation and delamination under aqueous conditions.⁽¹⁴⁻¹⁶⁾

Recently, liquid crystal polymer (LCP) has received increasing attention as a new material for biomedical applications, including cortical stimulators for pain control,⁽¹⁷⁾ retinal implants,⁽¹⁸⁾ and intraocular pressure sensors.⁽¹⁹⁾ LCP is a thermoplastic polymer consisting of rigid and flexible monomers, and are biocompatible, chemically inert,

and mechanically stable. The electrical and mechanical characteristics of LCP are summarized in Table 1 and compared with other conventional polymers for biomedical applications, such as parylene-C, polyimide and polydimethylsiloxane (PDMS).^(20–23) The most advantageous property of LCP as a packaging material for implantable neural prostheses is its extremely low moisture absorption rate ($< 0.04\%$) that is significantly lower than those of other biocompatible polymers such as polyimide ($\sim 2.8\%$) and parylene-C (0.06–0.6). The helium permeability of LCP has been reported as 2.19×10^{-11} cm²/s, which is comparable to 8.5×10^{-11} cm²/s for Corning 7740 glass.⁽²⁴⁾ A recent study has revealed that a helium leakage rate of 1×10^{-9} mbar-liter/s ($\sim 1 \times 10^{-9}$ atm-cm³/s) was measured for a 25- μ m-thick bulk LCP film, and less than 5×10^{-8} mbar-liter/s ($\sim 5 \times 10^{-8}$ atm-cm³/s) was measured from the LCP film with a feedthrough array; these values are comparable to the leakage rate of glass substrates with metallized vias.⁽²⁵⁾ These results directly showed that LCP is feasible as the packaging material of implantable neural prostheses if properly processed.

A LCP-based implantable system can be formed into a conformable structure that can fit the nonplanar surface of target tissues, by the thermoforming process. Three-dimensional structures of LCP films also can be constructed into a packaging structure to enclose the stimulator ICs and circuitries, because LCP can be thermoformed into the desired nonplanar shapes by applying heat and pressure with metal molds.⁽²⁶⁾ Although Young's modulus of commercially available LCP films, ranging from 2 to 10 GPa, is slightly higher than those of conventional polymer materials such as polyimide (~ 2.4 GPa) and parylene-C (~ 3.2 GPa), the stiffness of LCP can be overcome by conformable fabrication. The properties of LCP, such as melting temperature and coefficient of thermal expansion (CTE), can be modulated by varying the composition of additives during the film manufacturing process. Exploiting the different melting points of high-melting-temperature LCP films (310–335°C) and low-melting-temperature LCP films (280°C) enables them to be thermally bonded together without the use of adhesive materials, by utilizing the low-melting-temperature LCP films as bonding layers.

It is also highly advantageous that LCP is compatible with conventional micro-electromechanical systems (MEMS) technologies. Thus it is possible to make precise micron-scale features for the high-density microelectrode array and the interconnecting lines on the film by micromachining processes such as photolithography, metallization, and dry/wet etching.⁽²⁷⁾ Previous studies have revealed that LCP-based multielectrode arrays can be successfully fabricated with two layers of LCP films. This multilayered

Table 1
Properties of polymer materials used in biomedical implants.

	LCP ⁽²⁰⁾ (Vecstar)	Polyimide ⁽²³⁾ (PI2525)	Parylene-C ⁽²¹⁾ (GALXYL)	PDMS ⁽²²⁾ (Med-1000)
Melting temp. (°C)	280–335	> 400	290	—
Tensile strength (MPa)	270–500	128	69	6.2
Young's modulus (GPa)	2–10	2.4	3.2	0.1–0.5
Water absorption (%)	< 0.04	2.8	0.06–0.6	< 1
Dielectric constant (1 MHz)	2.9	3.3	2.95	2.6

structure has shown a good biocompatibility in rabbit retinal tissues for 4 months, and also much stronger adhesion between the layers compared with polyimides when examined after 8 weeks in 75°C PBS.⁽¹⁸⁾ In addition, LCP is suitable for RF applications because of its low dielectric constant and low dissipation factor in the range of GHz.^(28,29) LCP is, unlike titanium and other metals, radio frequency (RF) transparent, enabling the integration of power and data telemetry coils into one package. Embedding a coil into the system package and thus substituting the metal-based package by thin and flexible LCP allows the miniaturization of implantable devices as well as the reduction of the magnetic resonance imaging (MRI) artifact caused by RF scattering by a metal case. Previously, we showed that a thin and flexible planar coil can be microfabricated on the LCP substrate for power delivery and data transfer into the implanted devices, and its performance was verified under laboratory conditions as well as under *in vivo* conditions.⁽³⁰⁾

All of the advantages mentioned above can contribute to the implementation of a LCP-based monolithic retinal prosthetic device. The LCP-monolithic system is a one-body device made of a single material, where the electrode array, the RF coil, the package and the system substrate are integrated. Compared with conventional devices of metal- or ceramic-polymer hybrid, or all-polymer-based systems, this device features several merits including 1) a thin, flexible, and conformable device shape, 2) simple fabrication, and 3) long-term reliability.

In this study, therefore, we present two major advances for the LCP-based monolithic retinal implant. The first one is the spherical deformation of LCP-substrates with internal circuits and a planar coil printed on it, for the tight attachment of the system on the eyeball, as shown in Fig. 1. The other is the *in vitro* accelerated soak test to verify the long-term reliability of LCP-encapsulation and for comparison with conventional polymers including polyimide and parylene-C.

2. Materials and Methods

2.1 *Thin, flexible retinal implant*

The dimensions of the retinal implant can be reduced by employing LCP as the substrate as well as the packaging material. To achieve the minimized device and structural conformability, the novel retinal implant schematically depicted in Fig. 1 is proposed. The system package has the maximum thickness of 1.5 mm and diameter of 15 mm by monolithically encapsulating the system using LCP. A current stimulator application-specific integrated circuit (ASIC), and discrete components are assembled onto the “ceiling” of the domed package. Since LCP is transparent to RF, the coil for RF telemetry is also integrated into the package lid. There is no need to separate the package and the telemetric coil, unlike the metal-packaged system, which enables the minimization of the area of the device. The embedment of the coil does not increase the thickness of the system package as the coil is fabricated on the flexible LCP substrate by thin-film processes.⁽³⁰⁾

The entire system can be molded into a conformal shape to fit the curvature of the eyeball, through the thermoforming process. This device is designed to have a

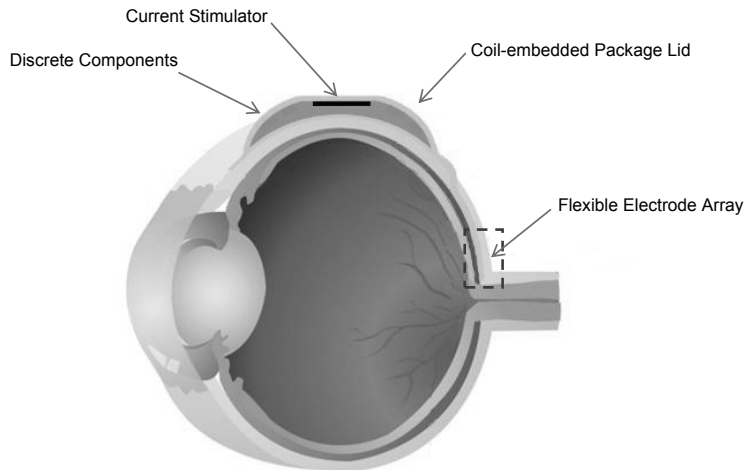


Fig. 1. Schematic diagram of LCP-based retinal implant attached to the surface of eyeball. The system package measures 15 mm in diameter and 1.5 mm thickness, and encases the current stimulator ASIC and several discrete components. The planar coil for power delivery and data transmission is also embedded into the package lid for minimizing the system size. The system is a monolithic system in which the entire system, including the package, the electrodes, and the coil, is fabricated on the single-body LCP substrate for higher reliability and simpler fabrication. The flexible electrode is inserted into the suprachoroidal space.

streamlined shape to minimize patient discomfort after it is attached on the surface of the eyeball, and thus to enhance the stability of long-term attachment. It is expected that this device will weigh approximately 0.3 g, including the package, electrode array, ASIC, and all the discrete components needed. The overall shape and the size of the proposed novel system is comparable to those of the Ahmed glaucoma valve (New World Medical, Inc., CA, USA), a medical shunt attached on the eye surface to reduce the intraocular pressure (IOP) in the treatment of glaucoma. The Ahmed valve (Model FP7, for adult) measures 13, 16, and 0.9 mm in width, length, and thickness, respectively,⁽³¹⁾ and weighs 0.25 g. The Ahmed valve is widely accepted to be stable in long-term attachment of more than 10 years.

2.2 Simplified fabrication and conformable structure

These fabrication processes can be simplified by employing the LCP films as a substrate for electrodes as well as the packaging material. The LCP system can be made of a single body of a single material, and in addition, most fabrication steps are batch processes of established semiconductor processes. The process is further simplified by integrating the telemetric coil into the package itself. These simpler fabrication processes can lower the manufacturing cost significantly. Therefore it is expected that

more potential beneficiaries will be able to afford the developed prostheses.

The LCP-based monolithically encapsulated retinal implant proposed in this research, shown in Fig. 1, is made from a single-body LCP substrate, removing the necessity of feedthroughs. Through the fusion-bonding process of LCP, the multilayered structure for the enhanced planar coil and circuit interconnection can be easily constructed. A LCP substrate for accommodating a stimulator ASIC for generating stimulation current, discrete components for surrounding circuitries, and the planar coil for transcutaneous power and data transmission, was fabricated on the multilayered LCP structure by industrial flexible printed circuit board (FPCB) technology (Flexcom, Ansan, Korea). Four metal layers were built by stacking two 50- μm -thick LCP films with metal cladding on both sides, and one bonding layer sandwiched between them. Two of four metal layers were for spiral coils and two layers for internal circuitries. The circular area of 5 mm diameter in the center of the substrate was maintained flat so that the stimulator ASIC of 3.3 mm \times 3.3 mm can be bonded by either wire bonding, flip-chip bonding using anisotropic conductive film (ACF), or ultrasonic bonding of Au bumps.

The thermoforming process of the LCP films followed, and a spherical curvature of the system package was realized so that the implant can be tightly attached on the surface of the eyeball and the package thickness can be minimized. The schematic process flow of the deforming process is depicted in Fig. 2. The alignment holes are created on the substrate by laser machining (Fig. 2(a)) and then fixed into a pair of aluminum molds by combining the alignment keys and alignment holes (Fig. 2(b)). The mold is heated

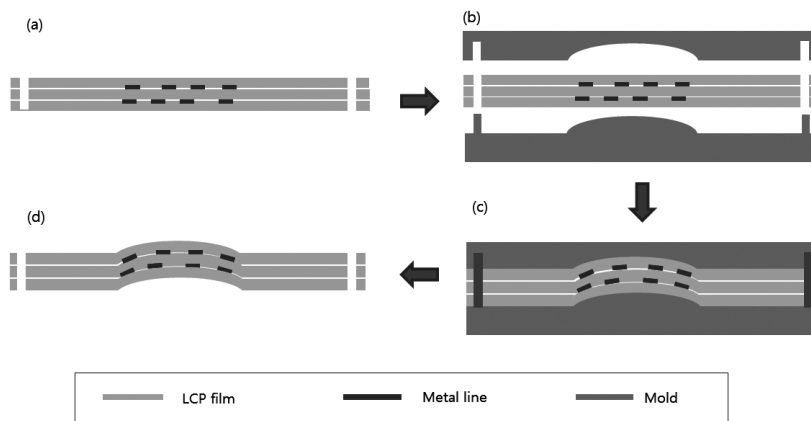


Fig. 2. Schematic diagram of the thermoforming process. (a) Alignment holes are created on the substrate by laser machining and (b) then fixed into the pair of aluminum molds. The substrate and the molds are aligned using alignment pins and holes. (c) LCP substrate is heated and pressed using a heat press and (d) then released after cooling. The 4-layer structure was simply depicted as a double-layered substrate in this figure.

to 230°C and maintained at that temperature for 20 min with compressive pressure (Fig. 2(c)). After cooling to room temperature, the pressure is lowered and the deformed substrate is released (Fig. 2(d)).⁽²⁶⁾

To ensure that the deformation process does not adversely affect the flexible circuits and substrates, the test patterns for the system circuit and the planar coil are fabricated on the LCP substrate. The electrical characteristics of circuits and the planar coil are evaluated before and after the forming process and compared. The transmission performance of the deformed planar coil is evaluated by connecting the coil to the current stimulator ASIC with peripheral circuitries on the custom-built printed circuit board. The criteria include the efficiency of power delivery and the maximum operating distance with which the stimulator can generate the desired current pulse without lack of power or unacceptable error rates.

2.3 Long-term reliability

The major advantage of using LCP lies in their superior long-term reliability over conventional polymer-based systems, while still maintaining the merits of polymers such as thinness, flexibility, and compatibility with thin-film semiconductor processes. Apart from the fabrication of eye-surface-conformable system substrates, we conducted an *in vitro* soak test to evaluate the durability of LCP encapsulation at the elevated temperature. The long-term reliability of LCP encapsulation has been investigated in a previous study.⁽¹⁸⁾ The LCP-based microelectrode array implanted in rabbit retina for two years showed no structural degradation, whereas considerable delamination and blistering were found from the polyimide-based electrode array. Lee *et al.* conducted an *in vitro* accelerated soak test of polymer materials by measuring the leakage current between insulated multi-interdigitated electrodes (MIDEs) immersed in 75°C phosphate-buffered solution (PBS).⁽²⁶⁾ The experimental setup is depicted in Fig. 3. The MIDE sample fabricated on the LCP substrate before and after encapsulation is shown in Fig. 3(a). Six interdigitated electrodes were located for each sample, where five of them were soaked (channels 1 to 5) and one of them (channel 4) remained above the soak level (Fig. 3(b)).

These MIDE arrays were encapsulated by another layer of LCP, and then placed in a bottle filled with PBS inside a convection oven at 75°C. A 5 V DC bias was momentarily applied for less than 10 min a day between the interdigitated electrodes (IDEs) to measure the leakage current with a picoammeter (Model 6485, Keithley Instruments, OH, USA). Leakage current increases as moisture and ions infiltrate into the encapsulated samples during the accelerated soak test. Identical MIDE patterns were fabricated using polyimide and parylene-C, and tested through the same procedure as for LCP to compare their long-term reliabilities.⁽²⁶⁾

In the present study, the *in vitro* soak test of the LCP-encapsulated samples is continued until the sample fails, which means that the leakage current exceeds the threshold level. The threshold current level for failure is arbitrarily set at 1 μ A based on our experience in preliminary measurements. The failed sample is harvested and investigated to elucidate the leakage path. Moreover, we here report the extended result from an *in vitro* soak test of an LCP-encapsulated sample soaked at 37°C.

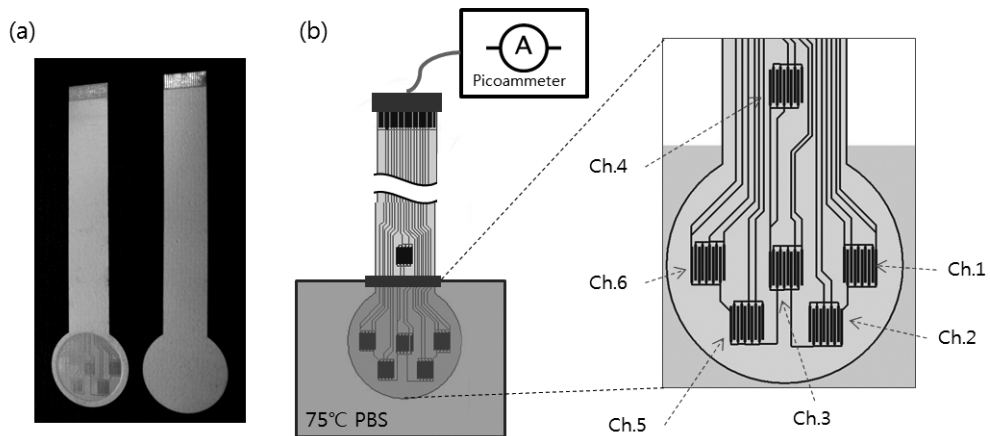


Fig. 3. Experimental setup for *in vitro* accelerated soak test for measuring electrical leakage current between IDE patterns to evaluate the reliability of LCP encapsulation. (a) Six IDE patterns are fabricated on the LCP substrate and laminated by thermal bonding and then immersed in 75°C PBS. (b) One of the six IDEs was located above the soaking level as a control, while five IDEs were soaked. Electrical current between the two terminals of IDE is maintained at a very low level if LCP encapsulation is intact, but leakage current increases when moisture penetration occurs.

3. Results

3.1 Substrate fabrication and conformal forming

A flexible LCP substrate was fabricated by integrating an ASIC, circuits, and a planar coil, as shown in Fig. 4. It consists of four metal layers: two layers for the circuit footprint and two layers for the planar coil. The electrical characteristics of the fabricated planar coil were measured with an impedance analyzer (Model 1260A, Solatron, UK). The inductance and resistance were 11.2 μH and 10.4 Ω , with a quality factor of 14.0. The inductive link composed of this planar coil and an external wire-wound coil was capable of transferring power and data to the stimulator ASIC as far as 20 mm away.

Figure 4 also shows the results of the thermoforming process giving a spherical curvature to the flexible LCP substrate. The diameter of the deformed structure is 15 mm and the height is approximately 3.5 mm, as depicted in Fig. 4(a). The footprint for electronics on the inner face of the domed substrate is shown in Fig. 4(b), along with the planar coil on the outer surface in Fig. 4(c). An exposed coil is shown for demonstration purposes, but it will be encapsulated in the LCP system in the actual device.

Table 2 summarizes the measurements of the electrical characteristics for the planar coil before and after the deformation process to reveal any adverse effect of the

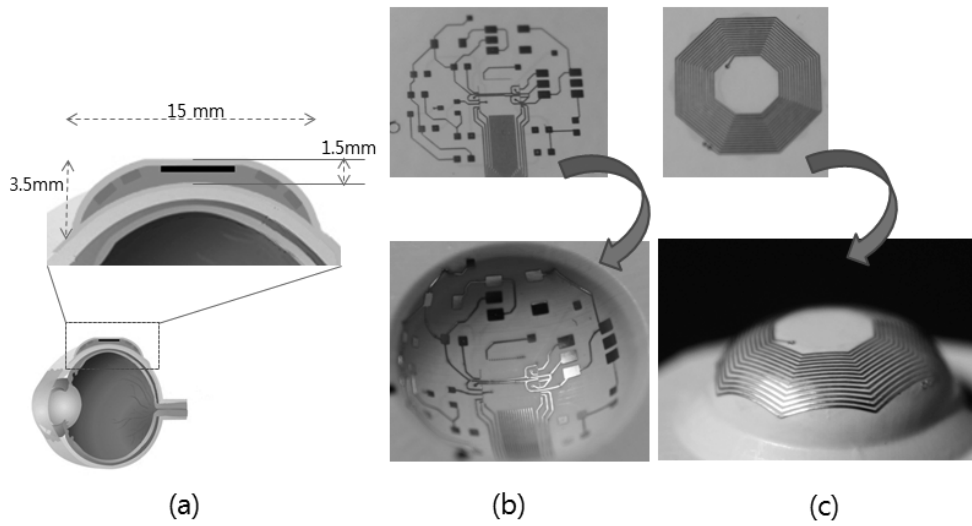


Fig. 4. Fabricated LCP-based substrate for accommodating IC, the discrete components, and the planar coil. (a) Dimensions and degree of curvature are described for the proposed human retinal implant system. The two sides of the LCP substrate, where the printed circuit board and the planar coil are formed, are shown in (b) and (c) before and after conformal forming. Their electrical connection of conducting lines and the functionality of the coil were confirmed after the deformation. The exposed planar coil in (c) is for demonstration purposes to show the intactness of the metal lines after deformation. In the actual device, the coil would be encapsulated in the LCP system package.

Table 2

Electrical characteristics and link performance of planar coil before and after the deformation process ($N = 4$).

	L (μH)	R (Ω)	Q (at 2.5 MHz)	Power efficiency (at 5 mm distance)	Maximum operating distance*
Before	11.2	10.4	14.0	30%	20 mm
After	10.8 ± 0.13	10.8 ± 0.14	13.4 ± 0.02	$30 \pm 0.03\%$	21 ± 0 mm

*Acrylic discs of 1 mm thickness were stacked to separate the coil pair, thus the operating distance was measured in 1 mm steps.

deforming process on the flexible electronics. The inductance and resistance of the deformed coil were $10.8 \pm 0.13 \mu\text{H}$ and $10.8 \pm 0.14 \Omega$, with a quality factor of 13.4 ± 0.02 , indicating that the electrical properties did not undergo any significant change (less

than 4%). The link performance, measured in terms of power efficiency and maximum operating distance of the stimulator circuit, also did not degrade after the deformation. The interconnection of circuit traces and footprints were confirmed to be intact by measuring the test circuits. The number of samples was 4 in this study.

3.2 Long-term reliability tests

Figure 5 shows the leakage current measured from six IDEs of the LCP-based sample soaked in 75°C PBS. After a rapidly increasing phase during the first 50 days, the stabilized leakage current remained in the order of 10^{-9} A for more than 300 days. However, after a certain time point, the leakage current from several channels suddenly jumped to the level of milliamperes, indicating that the insulation failed owing to moisture penetration. This test was repeated twice using two identical LCP-encapsulated test samples; one failed after 381 days and the other after 378 days in 75°C PBS. The LCP-encapsulated sample was found to have a higher reliability than polyimide- and parylene-C-encapsulated samples, which failed after 66 days and 117 days of soaking, respectively.⁽²⁶⁾

Considering that the channels located in the peripheral region (channels 1, 5, and 6) failed about 50 days prior to the inner channel (channel 3) and unsoaked channel (channel 4),

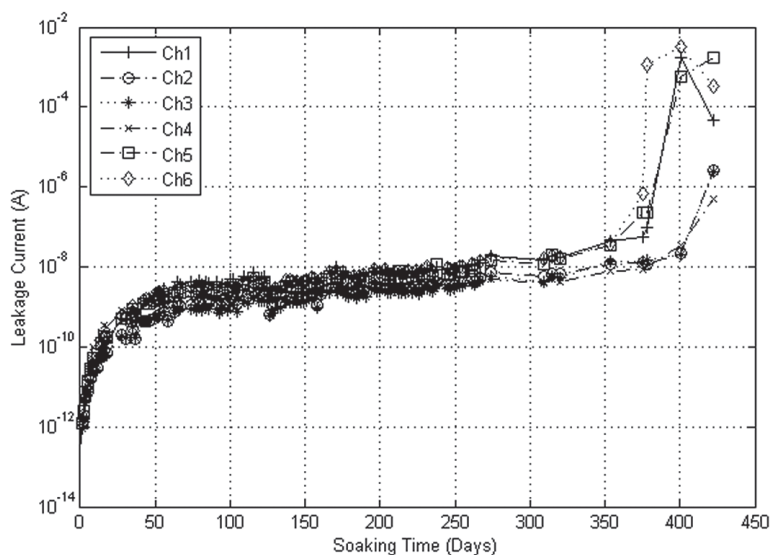


Fig. 5. Leakage current measured from 6 IDE patterns encapsulated by LCP soaked in 75°C PBS. The leakage current of 3 IDEs exceeded 1 mA after 380 days of soaking. 5 V was applied between the two terminals of IDEs during the current measurement using a Keithley 6485 picoammeter.

it is likely that the moisture penetrated from the sidewall of the sample and deteriorated the interlayer adhesion of LCP layers, rather than directly through the surface of LCP film. A drastic increase in leakage indicates that once the infiltrating moisture from the edge reaches the IDE pattern, it quickly spreads throughout the IDE pattern, presumably along the metal traces. This presumption can also explain the similar timing of failure at channels 3 and 4, which were in the center of the soaked part and the nonsoaked region, respectively.

The accelerated condition might be an unfavorable condition for LCP owing to thermoplasticity. Therefore, in addition to the accelerated soak test under 75°C, a nonaccelerated soak test at 37°C was conducted, and the result is plotted in Fig. 6. Experimental methods and the sample preparation were identical to those of the accelerated test except for the temperature of the PBS solution. It was observed that the leakage current from all the channels, except channel 1, remained below 0.1 nA for more than 500 days, despite some degree of fluctuation. Channel 1 failed after 470 days of soaking, which is an unexpected result, and further investigation is needed to determine the cause of this failure. This measurement is still ongoing.

The soaked LCP-based samples were harvested after they failed and visually inspected, as shown in Fig. 7. Delamination of multiple LCP films was observed, and the multiple layers could be separated by forceps. However, more severe signs such as

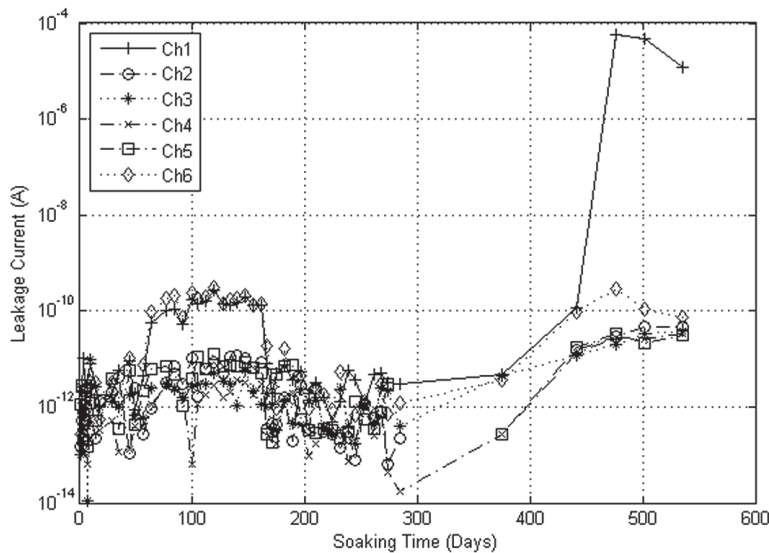


Fig. 6. Leakage current measured from 6 IDE patterns encapsulated by LCP soaked in 37°C PBS. Leakage currents from all the channels except channel 1 remained below 1 nA.

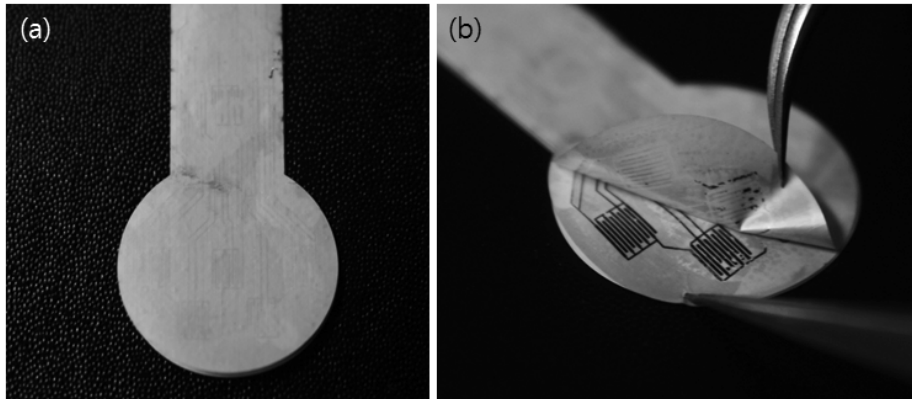


Fig. 7. Failed IDE sample encapsulated by LCP after soak test (a). When the leakage current dramatically increased, delamination between the LCP layers was observed (b), but no signs of dissolution, blistering, or corrosion were observed.

dissolution, blistering, and corrosion, which were observed for the failed polyimide and parylene-C,⁽²⁶⁾ were not observed for the failed LCP samples.

4. Discussion

4.1 *Advanced soak test*

In this study, the leakage current between the insulated MIDEs immersed in 75°C PBS was measured in the accelerated soak test. Even though this method was used in several studies previously, there is a limitation of using MIDEs because of the electrically passive system. An actual implanted device of a neural prosthesis is usually composed of active electronics such as an RF link, ASIC, and discrete components. To precisely investigate the encapsulation properties of polymers over a long period, the test should utilize active components generating electrical currents because the electrical field can enhance the degradation of polymers, particularly when thermal or mechanical stress exists. Accordingly, in order to evaluate the system reliability under conditions that mimic the actual implanted situation as closely as possible, the soak test of an LCP-encapsulated active system must be conducted with a continuously generated stimulation current. In addition, new IDE patterns are being designed for more effective leakage paths in the LCP-encapsulated package and LCP-insulated electrode with various sizes of site openings.

4.2 *Stiffness of LCP electrode array*

The slight higher stiffness of LCP might raise a concern about long-term stability and safety, particularly for delicate and soft tissue such as the retina. It was found that the

rigidity of the microelectrode array chronically implanted into the retinal space can lead to the detachment of the retinal layer in the worst case (unpublished data). In addition, if a stiff electrode array has difficulty in maintaining close contact with the curved retina, the efficiency of stimulation would be deteriorated owing to the increased distance between electrodes and target cells. This may result in an increased stimulation threshold as well as a lower visual resolution caused by current spreading.

This potential obstacle of the LCP-based retinal electrode, however, can be overcome by giving the electrode array a spherical curvature so that the electrode array can stably and safely retain a tight contact with the target cell layer. A conformable shape can be achieved through the thermoforming process after the fabrication of the whole electrode array. As described above, the system substrate also can be deformed into the conformal structure for realizing tight contact with the eyeball, by a thermoforming process with the application of appropriate heat and pressure using a metal jig and a heating press machine. However, although the forming process can mold the electrode into the desired three-dimensional structure, the optimal curvature must be carefully determined considering the variation among human subjects. An electrode array with a higher curvature than that of the outer surface of the eyeball can disturb the smooth electrode insertion through the retinal surface.

To verify the long-term stability of the proposed LCP-based electrode in the retinal space, prolonged implantation into a rabbit eye will be conducted and monitored periodically using optical coherence tomography (OCT) images for a period of more than 2 years. The optimization of the curvature given to the LCP-electrode head is also planned to achieve a tight contact with the target neurons and efficient stimulation, as well as minimized damage to retinal tissues.

5. Conclusion

A flexible and eye-surface-conformable multilayered monolithic retinal implant was developed using LCP substrates to integrate a current stimulator ASIC, surrounding electronics, a microelectrode array, and a planar transmission coil. The four-layered flexible substrate carrying ASIC, circuit footprints, and the planar coil was fabricated, followed by the thermal-forming process to achieve the conformable structure fitting the eyeball. It was confirmed that the deformation did not damage the flexible electronics by evaluating the electrical characteristics of circuits and the transmission performance of the planar coil after the heat-press process. The long-term reliability of LCP encapsulation was investigated through the *in vitro* accelerated soak test. The LCP-laminated sample could survive for 380 days in PBS at 75°C, indicating its superior durability compared with polyimide and parylene-C. It is speculated that the primary failure mechanism is moisture penetration through the interlayer adhesion. To verify this hypothesis, the interlayer adhesion will be reinforced and tested in a future work. The nonaccelerated soak test in PBS at 37°C currently exceeds 500 days, and is still ongoing. Taken together, the LCP-based monolithic retinal implants have several advantages compared with the current technologies, such as a thin, flexible, and conformable device shape, simple fabrication, and long-term reliability.

Acknowledgements

This work was supported in part by the Public Welfare & Safety research program through the National Research Foundation of Korea (NRF) funded by the Ministry of Education, Science and Technology (2011-0020987), in part by the Brain Korea 21 Project, the Department of Electrical Engineering, Seoul National University in 2011, in part by the project of the Global Ph.D. Fellowship conducted by National Research Foundation of Korea from 2011 (2011-0007411). This work was also supported by the Smart IT Convergence System Research Center funded by the Ministry of Education, Science and Technology as Global Frontier Project (SIRC-2011-0031866).

References

- 1 C. W. D. Dodds, Y. T. Wong, P. J. Byrnes-Preston, M. Rendl, N. H. Lovell and G. J. Suaning: Proc. 4th Int. IEEE Eng. Med. Biol. Soc. Conf. Neural Eng., Antalya, Turkey, 2009, pp. 88–91.
- 2 M. S. Humayun: Trans. Am. Ophthalmol. Soc. **99** (2001) 271.
- 3 E. T. Kim, C. Kim, S. W. Lee, J.-M. Seo, H. Chung and S. J. Kim: Invest. Ophthalmol. Visual Sci. **50** (2009) 4337.
- 4 D. B. Shire, S. K. Kelly, J. Chen, P. Doyle, M. D. Gingerich, S. F. Cogan, W. A. Drohan, O. Mendoza, L. Theogarajan, J. L. Wyatt and J. F. Rizzo: IEEE Trans. Biomed. Eng. **56** (2009) 2502.
- 5 P. Walter, Z. F. Kisvárdy, M. Görtz, N. Alteheld, G. Rossler, T. Stieglitz and U. T. Eysel: Invest. Ophthalmol. Visual Sci. **46** (2005) 1780.
- 6 J. D. Weiland, W. Liu and M. S. Humayun: Ann. Rev. Biomed. Eng. **7** (2005) 361.
- 7 E. Zrenner: Science **295** (2002) 1022.
- 8 K. Nakauchi, T. Fujikado, H. Kanda, T. Morimoto, J. S. Choi, Y. Ikuno, H. Sakaguchi, M. Kamei, M. Ohji, T. Yagi, S. Nishimura, H. Sawai, Y. Fukuda and Y. Tano: Graef. Arch. Clin. Exp. **243** (2005) 169.
- 9 M. S. Humayun, J. D. Weiland, G. Y. Fujii, R. Greenberg, R. Williamson, J. Little, B. Mech, V. Cimmarusti, G. Van Boemel, G. Dagnelie and E. De Juan Jr: Vision Res. **43** (2003) 2573.
- 10 T. Fujikado, M. Kamei, H. Sakaguchi, H. Kanda, T. Morimoto, Y. Ikuno, Ke. Nishida, H. Kishima, T. Maruo, K. Konoma, M. Ozawa and Ko. Nishida: Invest. Ophthalmol. Visual Sci. **52** (2011) 4726.
- 11 H. Gerding, F. P. Benner and S. Taneri: J. Neural Eng. **4** (2007) S38.
- 12 D. C. Rodger, A. J. Fong, W. Li, H. Ameri, A. K. Ahuja, C. Gutierrez, I. Lavrov, H. Zhong, P. R. Menon, E. Meng, J. W. Burdick, R. R. Roy, V. R. Edgerton, J. D. Weiland, M. S. Humayun and Y.-C. Tai: Sens. Actuators, B **132** (2008) 449.
- 13 T. Schanze, L. Hesse, C. Lau, N. Greve, W. Haberer, S. Kammer, T. Doerge, A. Rentzos and T. Stieglitz: IEEE Trans. Biomed. Eng. **54** (2007) 983.
- 14 R. Delasi and J. Russell: J. Appl. Polym. Sci. **15** (1971) 2965.
- 15 S. Murray, C. Hillman and M. Pecht: J. Electron. Packag. **126** (2004) 390.
- 16 E. M. Schmidt, J. S. McIntosh and M. J. Bak: Med. Biol. Eng. Comput. **26** (1988) 96.
- 17 C. J. Lee, S. J. Oh, J. K. Song and S. J. Kim: Mater. Sci. Eng., C **24** (2004) 265.
- 18 S. W. Lee, J.-M. Seo, S. Ha, E. T. Kim, H. Chung and S. J. Kim: Invest. Ophthalmol. Visual Sci. **50** (2009) 5859.
- 19 E. Y. Chow, A. L. Chlebowski and P. P. Irazoqui: IEEE Trans. Biomed. Circuits Syst. **4** (2010) 340.

- 20 Kuraray group, <http://www.kuraray.co.jp/en/> (accessed on 15 February 2012).
- 21 V&P Scientific, Inc., http://vp-scientific.com/parylene_properties.htm (accessed on 15 February 2012).
- 22 Nusil Silicone Technology, <http://www.nusil.com/products/Healthcare/Restricted/Adhesives.aspx/> (accessed on 15 February 2012).
- 23 HD Microsystems, http://hdmicrosystems.com/HDMicroSystems/en_US/ (accessed on 15 February 2012).
- 24 M. J. Chen, A.-V. H. Pham, N. A. Evers, C. Kapusta, J. Iannotti, W. Kornrumpf, J. J. Maciel and N. Karabudak: *IEEE Trans. Microwave Theory Tech.* **54** (2006) 4009.
- 25 V. Sundaram, V. Sukumaran, M. E. Cato, F. Liu, R. Tummala, P. J. Nasiatka, J. D. Weiland and A. R. Tanguay: *Proc. Electron. Compon. Tech. Conf.*, San Diego, 2011, pp. 1308–1313.
- 26 S. W. Lee, K. S. Min, J. Jeong, J. Kim and S. J. Kim: *IEEE Trans. Biomed. Eng.* **58** (2011) 2255.
- 27 R. N. Dean Jr, J. Weller, M. J. M. J. Bozack, C. L. Rodekohr, B. Farrell, L. Jauniskis, J. Ting, D. J. Edell and J. F. Hetke: *IEEE Trans. Compon. Packag. Technol.* **31** (2008) 315.
- 28 L. Frisk and E. Ristolainen: *Microelectron. Reliab.* **45** (2005) 583.
- 29 G. Zou, H. Grönqvist, J. P. Starski and J. Liu: *IEEE Trans. Adv. Packag.* **25** (2002) 503.
- 30 J. Jeong, S. W. Lee, K. Min, K. Eom, S. H. Bae and S. J. Kim: *Proc. 33rd Ann. Int. Conf. IEEE Eng. Med. Biol. Soc.*, Boston, 2011, pp. 1097–1100.
- 31 New World Medical, Inc., <http://www.ahmedvalve.com> (accessed on 15 February 2012).